SYNAPSE 59:445–457 (2006)

Basal Ganglia Neural Responses During Behaviorally Effective Deep Brain Stimulation of the Subthalamic Nucleus in Rats Performing a Treadmill Locomotion Test

LI-HONG SHI,[1] FEI LUO,[2] DONALD J. WOODWARD,[1,3] AND JING-YU CHANG[1,3]*
[1]*Department of Physiology and Pharmacology, Wake Forest University School of Medicine, Winston-Salem, North Carolina 27157*
[2]*Institute of Psychology, Chinese Academy of Science, Beijing 100101, People's Republic of China*
[3]*The Neuroscience Program, Wake Forest University School of Medicine, Winston-Salem, North Carolina 27157*

KEY WORDS Parkinson's disease; electrophysiology; substantia nigra pars reticulata; movement disorders; striatum; globus pallidus

ABSTRACT Deep brain stimulation (DBS) of the subthalamic nucleus (STN) is an effective treatment for Parkinson's disease (PD). In spite of proven therapeutic success, the mechanism underlying the benefits of DBS has not been resolved. A multiple-channel single-unit recording technique was used in the present study to investigate basal ganglia (BG) neural responses during behaviorally effective DBS of the STN in a rat model of PD. Rats underwent unilateral dopamine (DA) depletion by injection of 6-hydroxyDA (6-OHDA) into one side of the medial forebrain bundle and subsequently developed a partial akinesia, which was assessed during the treadmill locomotion task. High frequency stimulation (HFS) of the STN restored normal treadmill locomotion behavior. Simultaneous recording of single unit activity in the striatum (STR), globus pallidus (GP), substantia nigra pars reticulata (SNr), and STN revealed a variety of neural responses during behaviorally effective HFS of the STN. Predominant inhibitory responses appeared in the STN stimulation site. Nearly equal numbers of excitatory and inhibitory responses were found in the GP and SNr, whereas more rebound excitatory responses were found in the STR. Mean firing rate did not change significantly in the STR, GP, and SNr, but significantly decreased in both sides of STN during DBS. A decrease in firing rate in the contralateral side of STN provides neural substrate for the clinical observation that unilateral DBS produces bilateral benefits in patients with PD. In addition to the firing rate changes, a decrease in burst firing was observed in the GP and STN. The present study indicates that DBS induces complex modulations of the BG circuit and further suggests that BG network reorganization, rather than a simple excitation or inhibition, may underlie the therapeutic effects of DBS in patients with PD. **Synapse 59:445–457, 2006.**

INTRODUCTION

Deep brain stimulation (DBS) of the subthalamic nucleus (STN) and the globus pallidus internal (GPi) significantly alleviates syndromes of Parkinson's disease (PD) and reduces dopamine (DA) supplement-induced side effects (Ashkan et al., 2004; Durif et al., 2002; Vitek, 2002a). In spite of significant clinical benefits, the mechanism underlying the therapeutic effects of DBS for PD has yet to be clarified (Benabid et al., 2002; Dostrovsky and Lozano, 2002; Vitek, 2002b).

Contract grant sponsor: NIH; Contract grant numbers: NS-43441, NS 40628, TW-006144, NS-19608; Contract grant sponsor: National Natural Science Foundation of China; Contract grant numbers: 30170307, 30370461.

*Correspondence to: Dr. Jing-Yu Chang, Department of Physiology and Pharmacology, Wake Forest University School of Medicine. Winston-Salem, NC 27157, USA. E-mail: jchang@wfubmc.edu

Received 26 September 2005; Accepted 20 January 2006

DOI 10.1002/syn.20261

Published online in Wiley InterScience (www.interscience.wiley.com).

The classic basal ganglia (BG) thalamocortical circuit model provides a conceptual framework for illustrating the physiological effects of DBS (Albin et al., 1989; Alexander et al., 1990; Delong, 1990). Accordingly, degeneration of midbrain DA neurons, a hallmark of PD, results in a disruption of information flow in the BG circuit. The model predicts that DA depletion will produce increased activity in the output nuclei of the BG, such as the substantia nigra pars reticulata (SNr) and the GPi. Accordingly, DBS of either the STN or the GPi would be predicted to alleviate motor deficits by reducing activity in these regions. However, the results reported in recent electrophysiological studies of DBS of the STN have been inconsistent.

Both in vitro and in vivo studies have demonstrated inhibitory neural responses in the STN, the target area of high frequency stimulation (HFS) (Beurrier et al., 2001; Filali et al., 2004; Magarinos-Ascone et al., 2002; Meissner et al., 2005; Tai et al., 2003). Inhibition may be the result of a depolarization block or the action of release of GABAergic neurotransmission. Other studies have suggested that DBS may directly drive STN neurons into a high discharge rate and induce burst firing patterns (Do and Bean, 2003; Garcia et al., 2003). Inconsistent results have also been reported in studies of BG output nuclei. Inhibitory responses were observed in the SNr in anesthetized rat during HFS of the STN (Benazzouz et al., 1995, 2000; Tai et al., 2003), whereas increased activity was found in GPi neurons in behaving monkeys (Hashimoto et al., 2003). Additionally, in monkey, DBS of the GPi decreased neural activity in the ventral thalamic nucleus, which receives inhibitory projections from the GPi (Anderson et al., 2003). These results are consistent with the possibility that DBS may activate STN cell bodies and axons projecting to the GPi. Furthermore, it is also likely that DBS exerts opposite effects on cell bodies (inhibition) and axons (excitation). This interpretation is supported by the findings of a computation modeling study (McIntyre and Grill, 1999).

In addition to firing rate changes, firing pattern changes in the BG regions have been documented extensively in parkinsonian conditions. Burst and synchronized oscillatory firing patterns have been found in parkinsonian patients, as well as in animal models of PD (Brown, 2003; Goldberg et al., 2004; Raz et al., 2000; Wichmann and Delong, 1999). Likewise, behaviorally effective DBS reduces burst firing patterns and abnormal oscillation in the BG, which may account for the therapeutic effects of DBS (Hashimoto et al., 2003; Meissner et al., 2005).

In the present study, we used a multiple-channel single-unit recording technique to record single unit activity in four major BG regions during behaviorally effective DBS in a rat model of PD. This work tested the hypothesis that DBS modulates activity in BG circuitry and thereby enables normal motor activity. The effects of DBS on BG activity may be manifested by changes in both firing rate and firing patterns.

MATERIALS AND METHODS

Animals

Twelve male Sprague-Dawley rats, weighing 350–400 g, were used in the experiment. Animals were housed in a reversed dark–light cycle (lights off from 7.00–19.00 h). Animals were treated in accordance with the U.S. Public Health Service Guide for the Care and Use of Laboratory Animals.

Surgical procedures

Rats were anesthetized with ketamine (100 mg/kg, i.p.) and xylazine (10 mg/kg, i.m.). Two types of microwire arrays were used. For single-unit recording, eight stainless steel Teflon-insulated microwires (50 μm diameter, Biographics Inc., Winston-Salem, NC), soldered onto connecting pins on a headstage, were stereotaxically lowered bilaterally into the dorsal lateral striatum (STR), GP, and SNr. For simultaneous recording and stimulation, an array of 10 platinum–iridium microwires (50 μm diameter, Teflon coated, CA Fine Wire, Grover Beach, CA) was used; the additional two microwires (same as recording microwires) were used as stimulation electrodes. These arrays were implanted in the STN. The following stereotaxic coordinates for these BG regions were obtained from the atlas of Paxinos and Watson (1986): 0.5 mm anterior to Bregma (A), 3.7 mm lateral to the midline (L), 4.0 mm ventral to the dorsal surface of the brain (V) for the STR; 0.8 mm A, 3.5 mm L, and 6.0 mm V for the GP, −3.5 mm A, 2.5 mm L, and 7.2 mm V for the STN; and −5.4 mm A, 2.0 mm L, and 7.8 mm V for the SNr. In addition, two 26-gauge cannulae were implanted 2 mm above the middle forebrain bundle at −2 mm A, 2 mm L, and 5 mm V. The headstage was secured onto the rat's skull surface with dental cement with six anchoring screws (1 mm diameter). Animals received ampicillin (60,000 U, i.m.) before surgery to prevent infection. Animals were housed individually and allowed to recover from surgery for at least 14 days before being subjected to the experiment.

Apparatus and experimental procedures

Behavioral assessments in the treadmill locomotion task and electrophysiological recording commenced 14 days after surgery. Rats were trained to walk on the treadmill with 20 s long, alternating on and off cycles. The treadmill belt moved at 12 cm/s during the on cycles. In the control condition, the treadmill session lasted 1 h. Three to four training sessions were required for rats to acquire smooth, constant walking patterns throughout the session.

Rats received unilateral DA lesions after baseline data were collected in the control condition. Desipramine HCl (15 mg/kg, i.p.) was administered first, and 30 min later, 6-hydroxyDA (6-OHDA; 8 μg free base dissolved in 4 μl saline containing 0.2% ascorbic acid) was infused over 8 min into the region of the MFB via a 31-gauge needle. The injection needle was left in place for 2 min to allow the drug solution to diffuse into the brain.

The DBS experiment was performed at least 14 days after the lesioning surgery. Stimulation was delivered to the STN using pairs of platinum–iridium electrodes (50 μm in diameter) within the array in a bipolar configuration in 3-s on, 2-s off cycles during 20-s treadmill walking phases. Distance between the electrodes was around 250–500 μm and impedance of electrodes was around 200 kΩ. It is worth noting that cell body and axons may be affected to different degrees by DBS, when different electrodes are used. The electrodes used in our study are much smaller than the ones used in human (2 mm in diameter). Such smaller electrodes generate much higher current density that may more likely activate cell bodies than the bigger electrode used in human patients do (Lozano et al., 2002).

The stimulation parameters were as follows: 130 Hz, 60-μs pulse width, 50–175 μA generated by Accupulser A310 stimulator and A-365 stimulus isolation units (WPI Inc., Sarasota, FL). In later stages of the experiment, charge-balanced pulses (60-μs stimulation pulse counterbalanced by 1% current, 6 ms opposite current) were programmed into the DS-8000 digital stimulator and DLS-100 digital linear isolator (WPI Inc.). This charge-balanced pulse was delivered through platinum–iridium electrodes and incorporated to minimize tissue damage caused by HFS. Stimulation pulse was timed and triggered by the Magnet System Realtime Protocol program. Pulses were simultaneously sent to the preamplifier to shut down the input for 1 ms. Clamping the input of the preamplifier reduced stimulation-induced artifacts in some cases.

If stimulation delivered through wires 9 and 10 did not improve locomotion, different pairs of microwires were tested from 90 permutations of the array of 10 microelectrodes. In practice, every electrode was tested as either an anode or a cathode. No more than three microwires in any array were identified as effective stimulation electrodes, as defined by improvement of treadmill walking when active. During HFS, the remaining eight microwires were used to record neural activity in the STN stimulation site.

Electrophysiological recording

Extracellular recordings of the four BG regions were performed by connecting the implanted microwire assembly to a motor-assisted commutator via a FET headstage plug and a lightweight cable. The commutator was free to turn, permitting unrestricted movement of the animal. Neuroelectric signals were passed from the headset assemblies to programmable preamplifiers, filters (0.5–5 kHz), and a multichannel spike-sorting device that timed spike with a 1 kHz resolution (Plexon Inc., Dallas, TX). As many as 62 neurons from the STR, GP, STN, and SNr were monitored simultaneously from 64 microelectrodes. Spikes were considered valid when the ratio of spike size to baseline noise was greater than 3. Spike activity and treadmill operation were recorded and controlled with the data acquisition software Magnet (Biographics Inc.).

Histology

At the conclusion of the final experimental session, each animal was subjected to the same anesthesia as in surgery. A positive current of 10–20 μA was passed through selected microwires for 10–20 s to deposit iron ions. Animals were then killed and perfused intracardially with 4% paraformaldehyde solution. Coronal sections (45 μm thick) were cut through the STR, GP, STN, and SNr and mounted on slides. Mounted sections were incubated in a solution containing 5% potassium ferricyanide/10% HCl to reveal iron deposits (recording sites) in the form of blue dots where the stainless steel microwires had been located. For localization of the platinum–iridium microwires, electrode tips were visualized as a lesion spot with neutral red staining. Boundaries of the four brain areas were determined with reference to the rat brain atlas of Paxinos and Watson (1986).

Data analysis

Data were processed off-line with Stranger (Biographics Inc.) and Nex programs (Plexon Inc.) for basic analysis and graphics; MatLab (Mathworks Inc., Natick, MA) and SPSS (SPSS Inc., Chicago, IL) were used for additional statistics. HFS generated considerable stimulation artifacts within the stimulation area and its surroundings. To eliminate the stimulation artifacts, 2-ms bins immediately following the onset of stimulation were deleted, and data were then merged in MatLab to fill the resultant 2-ms gaps. Recording channels with a stimulation artifact longer than 2 ms were not included in the final data analysis. Such artifact deletion resulted in a loss of nearly 25% of the bins during 130-Hz stimulation, but otherwise allowed artifact data to be studied, except for burst recognition algorithms that required temporal continuity. To compare the responses within neurons between the control and stimulation trials, computer-generated events (CGE) with the same frequency as that of the stimulation (130/s) were created during the treadmill walking phase in the trials without HFS, and 2-ms bins were deleted around these events and the data were merged.

In this way, control histograms were created for comparison with the data collected during behaviorally effective HFS. Raster and perievent histograms were plotted using the onset of treadmill, 3-s stimulation cycle, stimulation pulses, and CGE as references to compare neural activity in DBS and control conditions.

A sliding-window method was used to compare neural activity changes during HFS trials with that during control trials within the same session (see Schultz and Romo, 1992 for details). Briefly, counts per bin (from 1- to 100-ms bin size depending on the duration of analysis) of single neuron activity during control and HFS conditions were calculated for each trial. Neural activity in different conditions was then compared by a time window (from 3 ms for interpulse interval to 1 s for treadmill walking) moving at 1 to 300 ms s steps across the period of interest. Significant difference was detected when three consequent steps showed significant different level at $P < 0.05$ (student's t-test).

The following two criteria were used concurrently to detect significant changes in neural firing rates associated with behavioral events: (1) Firing rate changes (increase or decrease from baseline control in resting condition) of greater than 20% during the time periods of interest, such as tone and treadmill walking responses; (2) Analyses of differences in at least three successive steps of the moving window reached a statistically significant level ($P < 0.05$, student's t-test). These measures account for both slow and fast firing neurons and enable detection of both substantial (>20%) and significant (<0.05) changes. Burst analysis was performed in the Nex program based on the method of "surprise" (Legendy and Salcman, 1985).

Frame by frame video analysis (33 ms resolution) of limb movement during treadmill locomotion was conducted. Two limb movement events were identified by video analysis: footfall, defined as the initial paw contact with the floor, and foot off, defined as the paw leaving the floor (Cohen and Gans, 1975). To allow a more descriptive analysis, the step cycle was divided into two major phases: stance phase (when the paw was in contact with floor) and swing phase (when the paw was in the air), which were defined by the onsets of footfall and foot off, respectively (West et al., 1990). All timestamps for limb movement were compiled and entered into the data file as event nodes.

Treadmill locomotion was analyzed quantitatively by video analysis performed off-line in intact, DA-lesioned and DBS + DA-lesioned conditions. It should be noted that each rat served as its own control. That is, the rats' behavior was compared among three conditions: intact (baseline locomotive behavior before lesion), DA lesioned (postlesion in the absence of HFS), and DBS + DA lesioned. Analyses of variance (ANOVAs) with condition as the independent variable (3 levels) were used to detect significant differences in the behavioral data.

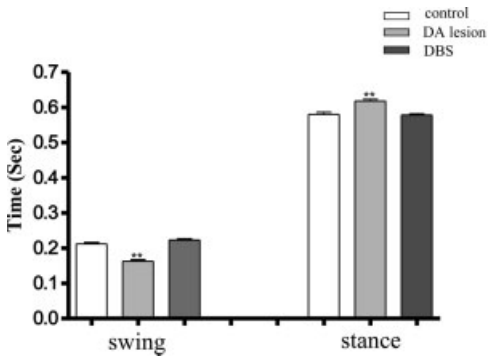

Fig. 1. Effects of DBS of the STN on treadmill locomotion. Locomotor activity was assessed by swing and stance times. Unilateral DA-lesioned rats exhibited akinesia during treadmill locomotion. A significant decrease in swing time and increase in stance time were observed in the DA-lesioned condition. DBS restored swing and stance times to control levels. (**$P < 0.01$, ANOVA).

RESULTS

Behavioral effect of HFS in the STN during the treadmill locomotion task

Treadmill locomotion tests were employed to determine the effects of the unilateral DA lesion on motor functions. Neurologically intact rats walked actively and smoothly during the treadmill-on phase for the entire 60-min session. After the lesion, however, rats exhibited onset of motor deficits at varying times ranging from 5 to 15 min into the test session. The typical motor deficit was characterized by slow and passive stepping on the treadmill. As a result, the rat was pushed back to the rear wall of treadmill chamber by the running treadmill. HFS of the STN induced immediate improvements in treadmill locomotion in the unilateral DA-depleted rats. The lesioned rats resumed normal walking patterns during HFS, as characterized by active, smooth steps that carried the rat toward the front part of treadmill chamber.

Analysis of swing and stance time of the outside (right) forelimb revealed that the DA lesion produced a decrease in swing and an increase in stance time (Fig. 1; $P < 0.01$). These changes in swing and stance time might reflect akinesia induced by DA depletion. Lesioned rats had difficulty initiating movement, which resulted in a longer stance time. On the other hand, the forelimbs had to swing faster to catch up with the treadmill, which resulted in a shorter swing time. Walking speed and number of steps were similar in both conditions because of a constant treadmill speed. Effective DBS in the STN completely restored normal walking patterns. During HFS, swing and stance times returned to control levels (Fig. 1). Electrophysiological data presented in this present study were collected exclusively from the session in which HFS of the STN significantly improved treadmill locomotion performance.

TABLE I. Neural responses in different basal ganglia regions during behaviorally effective deep brain stimulation of the STN

			Episode							
			20 s		10 s rest		3 s on		2 s off	
Side	Total no. of neurons	+/−	*N*	%	*N*	%	*N*	%	*N*	%
STR										
ipsi	63	+	12	19	1	1.6	10	15.9	6	9.5
		−	6	9.5	3	4.8	10	15.9	4	6.3
contra	62	+	8	12.9	0	0	6	9.6	4	6.4
		−	2	3.2	0	0	2	3.2	2	3.2
GP										
ipsi	60	+	6	10	0	0	4	6.7	5	8.3
		−	5	8.3	0	0	7	11.7	2	3.2
contra	56	+	1	1.8	0	0	1	1.8	0	0
		−	6	10.7	0	0	9	16	2	6.3
SNr										
ipsi	65	+	13	20	2	3.1	13	20	5	7.7
		−	12	18.5	2	3.1	14	21.5	2	3.1
contra	53	+	2	3.7	0	0	1	0.5	2	3.7
		−	4	7.5	0	0	4	7.5	2	3.7
STN										
ipsi	63	+	2	3.2	1	1.6	2	3.2	3	4.8
		−	39	62	9	14.3	41	65	9	14.3
contra	46	+	3	6.5	0	0	4	8.7	4	8.7
		−	12	26	0	0	11	23.9	2	4.3

+, − indicates excitatory and inhibitory responses, respectively.
20 s, 20 s treadmill on phase; 10 s rest, 10 s treadmill off phase; 3 s on, 3 s stimulation-on phase; and 2 s off, 2 s stimulation-off phase.

Neural responses in the BG with HFS of the STN during the treadmill locomotion task

In parallel with the behavioral improvement, HFS elicited a variety of neural activity changes in the BG regions. A total of 125 STR, 116 GP, 118 SNr, and 109 STN neurons were recorded during behaviorally effective HFS of the STN. Stimulation artifacts were monitored in the oscilloscope and recorded in the waveform files. Most of the stimulation artifacts in the STN, the site of stimulation, were less than 2 ms. Deletion of the 2-ms bins containing the stimulation artifacts, with subsequent data merging, did not substantially alter the calculated firing rate of the experimental or control data.

Stimulation-induced neural responses, as changes in mean firing rate, were evaluated during the 3-s stimulation-on and 2-s stimulation-off periods in the treadmill walking phase and during the 20-s resting periods. HFS of the STN frequently induced responses during the stimulation-on periods. Fewer responses were observed during stimulation-off periods. Activity during the off periods included persistent responses that continued throughout the entire off period, as well as transient rebound responses triggered by the termination of HFS. Persistent responses sometimes extended into the 20-s resting period. Such cells were most likely to be observed in the STN stimulation site. A summary of the neural responses is depicted in Table I.

Effects of HFS of the STN on STN neural activity

Behaviorally effective HFS of the STN induced predominant inhibitory neural responses in surrounding STN neurons (Fig. 2). Thirty nine out of 65 ipsilateral STN neurons (62%) were inhibited during the 3-s stimulation periods. Nine of these 39 neurons (23%) exhibited lasting inhibitory responses that extended into the 20-s resting period in the absence of active HFS (Fig. 3). Only 2 neurons (3.2%) increased their discharge rates during HFS. Another 2 neurons exhibited rebound excitation during the 2-s stimulation-off period and one of them also had an increased firing rate during the 20-s resting period when the HFS was turned off. Fewer neurons in the STN contralateral to the stimulation exhibited inhibitory responses during HFS (26%) relative to ipsilateral neurons. Excitatory responses were observed more often in the contralateral side (6.5%) than in the ipsilateral side of the STN. However, the mean firing rate decreased during DBS in both ipsilateral and contralateral side of the STN (Fig. 6).

Effects of HFS of the STN on SNr neural activity

Nearly equal numbers of neurons exhibited excitatory and inhibitory responses (around 20% each) in the ipsilateral SNr during STN stimulation. As a result, the mean firing rate did not change significantly during DBS (Fig. 6). Unlike those observed in the STN, the neural responses (changes in firing rate) in the SNr were mostly confined to the 20-s treadmill walking period. Few excitatory and inhibitory responses (3% each) were observed during the 20-s resting period in the ipsilateral SNr. Only one out of 65 cells exhibited rebound excitation during the 2-s stimulation-off period. Figure 4 depicts SNr neural responses during behaviorally effective HFS. Substantially fewer neurons in the contralateral side of the SNr responded to the HFS of the STN during the 3-s HFS-on period.

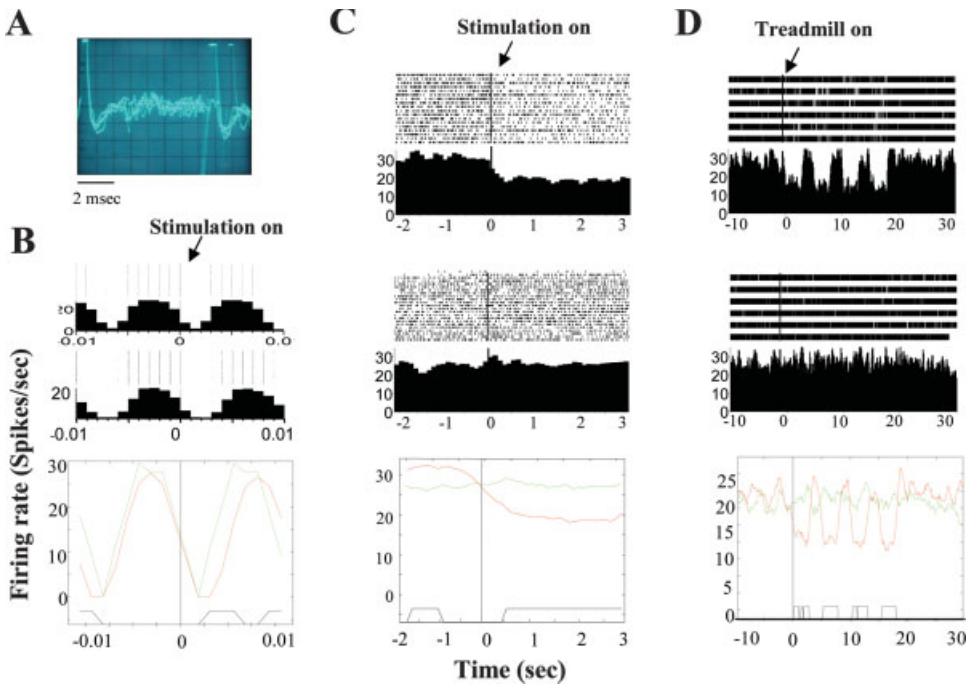

Fig. 2. STN neural responses during behaviorally effective HFS of the STN in an unilateral DA-lesioned rat. (**A**) Stimulation artifacts in a STN neuron near the stimulation site. The artifact duration was <2 ms in this case, and the corresponding 2-ms bins were deleted following stimulation pulses. The same deletion was also made in the control data. (**B**) A decrease in firing rate during 8-ms interstimulation pulse intervals was found in this STN cell. A raster and perievent histogram is shown in the top (with stimulation pulse delivered at 0 point) and middle (control condition without stimulation, 0 point marked computer generated events, CGE, at 130 Hz) rows, and a comparison between the stimulation and nonstimulation conditions is shown in the bottom panel. The marker on the abscissa in the bottom row indicates a statistically significant difference in spike rate at $P < 0.05$ (student's *t*-test). (**C**) Neural responses during the 3-s on, 2-s off stimulation cycle. A significant decrease in firing rate was observed during the 3-s stimulation-on period (top row, stimulation started at 0 point) in comparison with that of nonstimulation conditions (middle row, CGE, matching stimulation-on at 0 point). (**D**) Neural responses during the 20-s treadmill walking phase. The treadmill was turned on from 0 to 20 s and HFS was delivered in 3-s on, 2-s off cycles during each 20-s treadmill on phase. A significant decrease in firing rate was observed when the stimulation was turned on (top row), and spike discharges rebounded briefly following the termination of stimulation (bottom row).

Among the responding neurons, inhibitory responses outnumbered excitatory responses at a ratio of 4:1 (7.5% and 1.9%, respectively). The mean firing rate in the contralateral side did not change significantly during DBS (Fig. 6).

Effects of HFS of the STN on GP neural activity

Overall, less neurons in the GP (<20%) showed responses to HFS of the STN. The majority of responding neurons showed inhibitory responses during the 3-s stimulation period. Among excitatory response neurons, more cells exhibited rebound excitation during the 2-s stimulation-off period (around 8.3%) than during the 3-s stimulation period (6.7%). Unlike other regions, no cells in the GP exhibited lasting responses beyond the 20-s walking/stimulation period.

Effects of HFS of the STN on STR neural activity

In the side ipsilateral to the HFS, an equal number of neurons showed excitatory and inhibitory responses during the 3-s stimulation period (around 16% each). Six neurons (9.5%) had transient rebound excitation during the 2-s stimulation-off period (Fig. 5A). Two distinct patterns of inhibitory responses (short and long duration) were observed. Four out of 10 inhibitory response neurons exhibited short latency responses that lasted less than 1 s during the 3-s stimulation period. Because of their short duration, such inhibitory responses were not detected during the 20-s walking period. In contrast, 3 out of 10 inhibitory neurons exhibited lasting responses that extended into the 20-s resting period (Fig. 5B). In the side contralateral to the HFS, more excitatory responses were observed during both the 3-s stimulation-on and 2-s stimulation-off periods. However, like other BG regions, no response was found during the 20-s resting period in the STR contralateral to the HFS.

Effects of DBS on average firing rate in different BG regions are shown in Figure 6. No significant changes in firing rate could be detected in the STR, GP, and SNr. In the STN, mean firing rate in both stimulation and contralateral sites decreased significantly during DBS.

Changes in burst firing patterns during behaviorally effective HFS of the STN

Deleting the 2-ms time periods during the stimulation artifacts, as performed in firing rate analysis, resulted in a significant increase in burst rate in the control

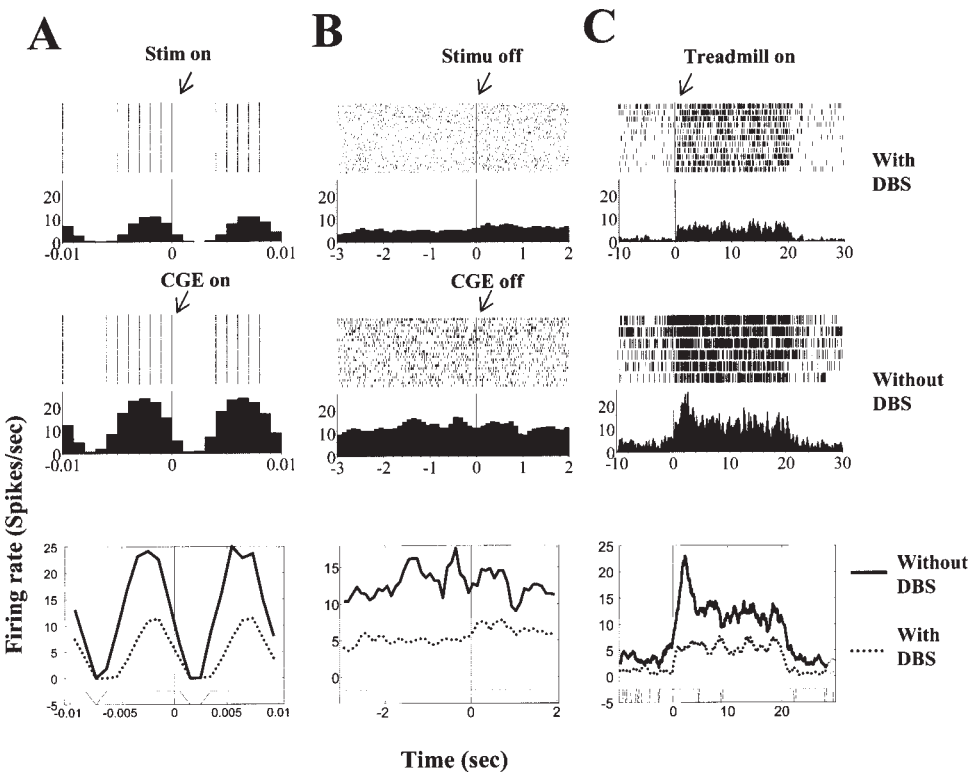

Fig. 3. Long lasting inhibitory responses were found in STN neurons surrounding the HFS site. This cell showed an inhibitory response during the interstimulation pulse interval (**A**), that persisted throughout an entire 3-s on, 2-s off stimulation cycle (**B**), and then extended well into the subsequent 10-s resting period, during which there was no stimulation (**C**). Top row: neural response during DBS. Middle row: neural responses during control condition without stimulation. Zero points in (**A**) represent stimulation pulses in DBS condition and computer generated matching events (CGE) in control condition. Zero points in (**B**) mark turning off of stimulation and CGE during 3-s on 2-s off stimulation cycles in DBS and control conditions, respectively. Zero points in (**C**) mark the start of 20-s treadmill walking phase.

condition (Fig. 7), making this method invalid for burst analysis. To obtain useful information, burst activity was analyzed during the 2-s stimulation-off period between each 3-s HFS train, since the improvement in motor performance was found to extend into this period. As demonstrated in Figure 7, cut and merge 2-s segments did not compromise the integrity of data for burst analysis. However, an obvious caveat for such data selection is that any changes in burst firing pattern during the stimulation period cannot be detected. Burst firing patterns were evaluated by surprise methods (Legendy and Salcman, 1985). Burst rate and percentage of spikes in burst were calculated using surprise 3, a level of statistic significance at which the burst activity was detected at a chance of less than 0.1% of the Poisson distribution. In comparison with control conditions, behaviorally effective HFS of the STN significantly reduced burst rate and percentage of bursting spikes in the STN and the GP. Figure 8 demonstrates the occurrence of burst events during the 2-s stimulation-off period in a STN neuron. The discharge rate of this neuron did not change during HFS, although the burst spikes were substantially reduced. Figure 9 summarizes the changes in burst firing patterns during behaviorally effective HFS by BG region. A significant decrease in burst firing rate and percentage of bursting spikes were found in the STN and GP during behaviorally effective HFS of the STN. On the other hand, the burst firing pattern remained unchanged in the STR and SNr during the HFS of the STN.

Histological localization of recording sites

Anatomic location of recording electrodes were revealed by potassium ferrocyanide and neutral red stainings of the tip of electrodes. All neurons included in this report were localized to the respective nuclei. Figure 10 illustrates the anatomic locations of the recording electrodes from which data are reported in this study. Data from electrode tips outside designated areas was not included.

DISCUSSION

The present study examined BG neural responses during behaviorally effective DBS of the STN in a rodent model of PD. Local inhibition seems to be the predominant neural response during behaviorally effective HFS in the STN. The responses in other BG regions were more complex; both inhibitory and excitatory responses were observed. In addition, decreases in burst firing were observed in the GP and STN. These results suggest that a continuous modulation of the BG network, rather than a simple excitation or inhibition, may account for the therapeutic effects of DBS in PD patients and PD animal models.

Compared with studies using anesthetized animals and in vitro slice preparations, the major advantage of the present study is that it identified BG neural responses to DBS that induced behavioral benefits in a rodent model of PD. We have recently established two rodent models of DBS, one is the treadmill locomotion

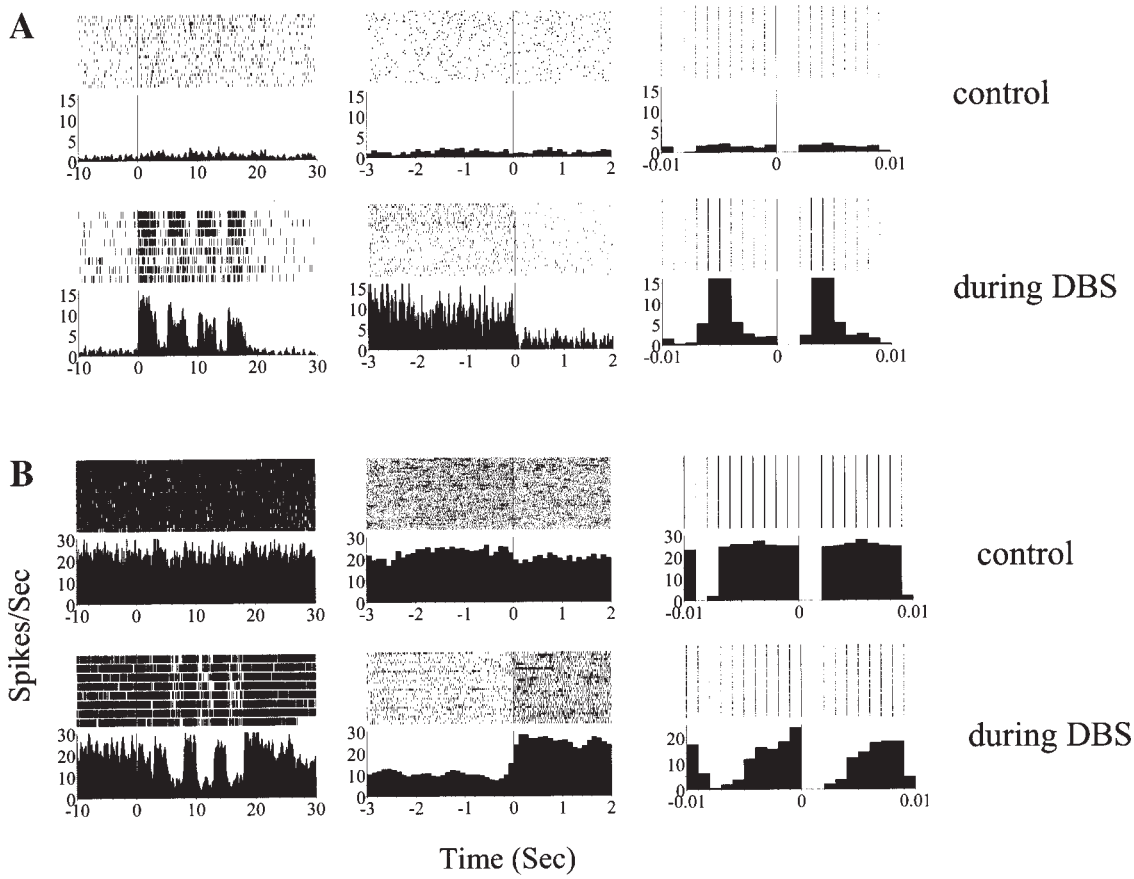

Fig. 4. Different neural responses in the SNr during behaviorally effective HFS of the STN. (**A**) A SNr cell showed excitatory response during HFS of the STN. The excitatory response was found during the 20-s treadmill walking phase (left panel, treadmill started at 0 point), the 3-s stimulation-on period (middle panel, stimulation-on at −3 s), and during interstimulation pulse intervals (right panel, stimulation pulses and corresponding CGE started at 0 point). (**B**) Another SNr cell exhibited inhibitory responses during HFS of the STN. The inhibitory responses were again observed throughout the 20-s treadmill walking phase (left panel), during the 3-s stimulation-on phase (middle panel), and the interpulse interval (right panel).

model employed in the current study (Chang et al., 2003), and the other is the limb use asymmetry model (Shi et al., 2004). Our previous report assessed treadmill locomotion performance using the animal's body position in the treadmill chamber. More accurate measurements were employed in the present study to better characterize DA depletion-induced treadmill motor deficits and the effects of DBS on motor performance. To accomplish this, we carefully evaluated step cycles using off-line video analysis. A significant decrease in swing time was found following the DA lesion, perhaps reflecting a sign of akinesia in the affected limb (contralateral to the lesion). The rats had difficulty initiating steps with the affected limb, which resulted in short and irregular steps. To compensate for these deficits, rats swung their unaffected limb (ipsilateral to the lesion) faster, which resulted in a decrease in swing time, and with large steps, which resulted in an increase in stance time (Chang et al., 2005). DBS of the STN completely restored normal locomotor function and brought the swing and stance times to the control level.

In the present study, profound inhibitory responses were observed in the STN stimulation site. A variety of STN neural responses have been documented during HFS using in vitro slice or isolated cell preparations. Some have reported an inhibition of STN neurons and attributed it to the inactivation of Na^+ channels (Beurrier et al., 2001; Magarinos-Ascone et al., 2002). Others have demonstrated an activation of STN neurons via a direct action on the neural membrane (Garcia et al., 2003). In addition, the observation of an excitatory response followed by an inhibitory response has been reported (Lee et al., 2003). Such variable results can likely be attributed to differences in stimulation parameters and experimental preparations. The data nevertheless provide critical insight into the cellular and molecular mechanisms underlying the effect of DBS. An important question is whether results obtained in vitro can be translated into the intact brain circuit and whether they are pertinent to therapeutic DBS used in clinical treatment. With such significant differences in experimental conditions, it is difficult to compare our results directly with those obtained from

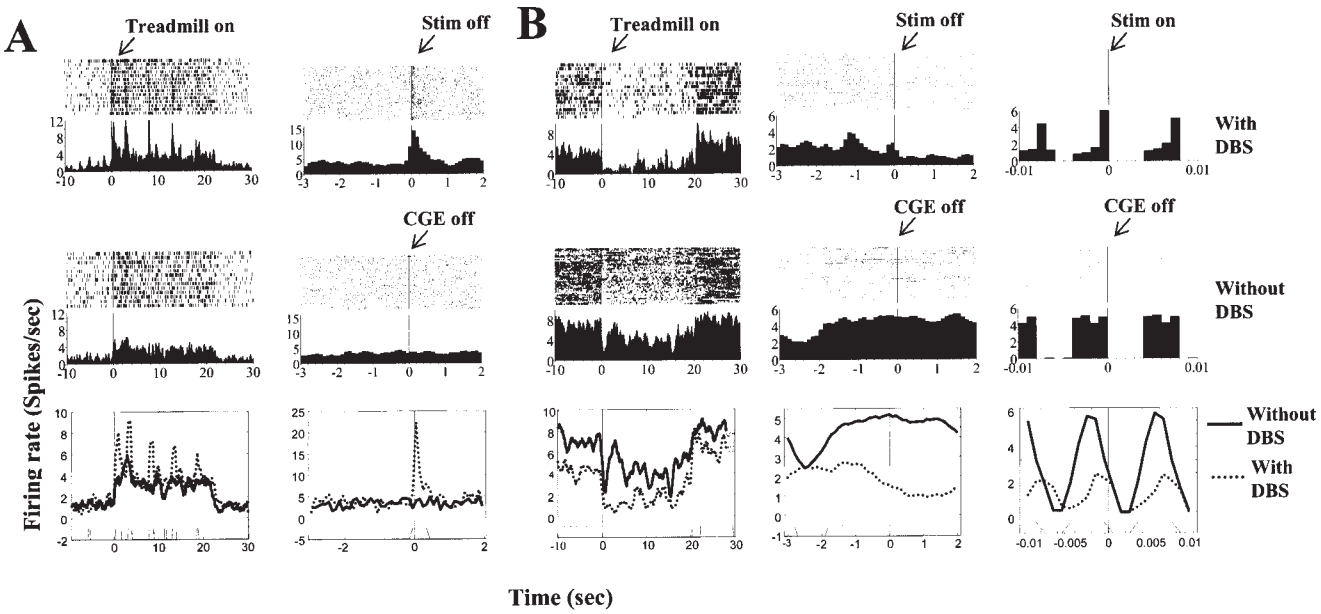

Fig. 5. Different neural responses in the STR during behaviorally effective HFS of the STN. (**A**) A transient rebound excitation appeared in this STR neuron at the termination of 3-s stimulation trains. Left panel: Neural responses during treadmill (from 0 to 20 s) with (top row) and without (middle row) DBS. Plot in the bottom row shows the comparison between the two conditions. Note transient rebound occurred at the end of each 3-s stimulation cycle. Right panel: raster and perievent histogram during 3-s on 2-s off stimulation cycles. Transient responses (<200 ms) took place at the end of 3 s stimulation. (top row). (**B**) A STR neuron exhibited long-lasting inhibitory responses. Left panel: Neural responses during treadmill (0–20 s) with (top row) and without (middle row) DBS. The inhibition extended into entire trial, including 2-s stimulation-off and 20-s resting periods (bottom row for comparison). Middle panel: Neural responses during 3-s on and 2-s off stimulation cycles. DBS (at −3 s) induced inhibition extended into 2-s stimulation-off period (bottom row for comparison). Right panel: Neural responses during interpulse intervals with (top row) and without (middle row) DBS. Profound inhibition occurred during 8-ms interstimulation pulse intervals (bottom panel for comparison).

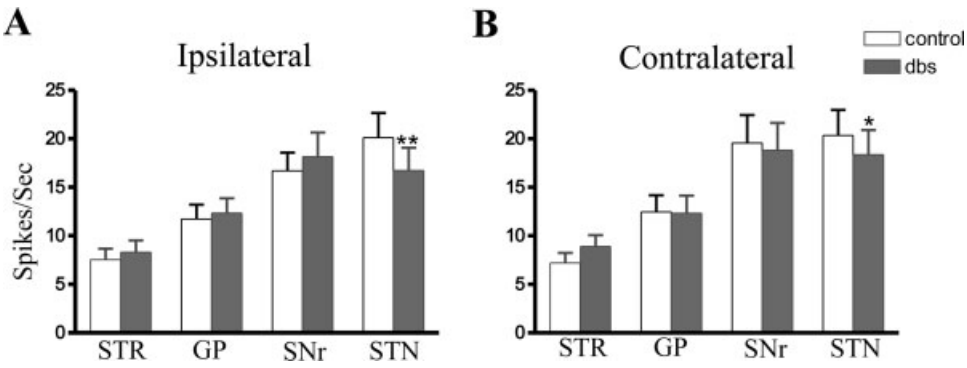

Fig. 6. Mean firing rate in different BG regions during control (without DBS) and DBS sessions in ipsilateral (**A**) and contralateral (**B**) sides. Significant decrease in firing rate was found in both side of the STN (*$P < 0.05$, **$P < 0.01$, student's *t*-test).

in vitro studies. On the other hand, our results agree very well with findings obtained from similar experimental conditions in human patients with PD, in which predominantly inhibitory responses have been reported in the stimulation sites of both the GPi and STN (Dostrovsky et al., 2002; Filali et al., 2004; Welter et al., 2004).

Observations of behaviorally relevant, predominantly inhibitory responses support the idea that stimulation may mimic lesion effects and thus inactivate cells in the stimulation sites. However, due to the stimulation artifact associated with DBS, we cannot exclude the possibility that HFS may act directly on the cell membrane of surrounding neurons and thereby drive them directly into high frequency firing (Garcia et al., 2003), given the fact that STN neurons are capable of firing at very high discharge rate (Kitai and Kita, 1987). It is worth noting that a recent study in the MPTP-treated monkey revealed time-locked multiphase responses in GP neurons during local HFS (Bar-Gad et al., 2004). The results point to a complicated reshaping of neuron activity in the stimulation site. The different cell types (glutamatergic STN cells vs. GABAergic GP cells) and stimulation parameters (60 μs in our study vs. 200–400 μs pulse width) may contribute to differences in the responses observed between the studies.

It is of interest to notice that unilateral DBS of the STN induces bilateral inhibitory responses in the

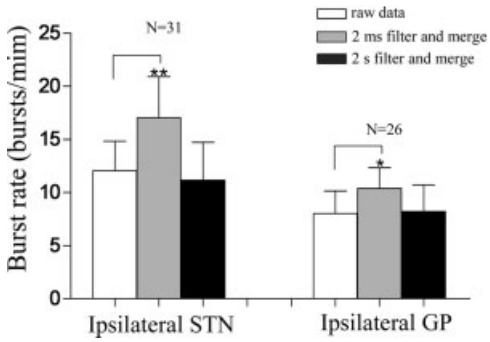

Fig. 7. Burst rate obtained from raw data and from data with different filter methods. STN and GP neurons in the ipsilateral site of lesion obtained from nine and six rats, respectively, during treadmill locomotion were used in the analysis. The same neurons were analyzed as raw data (without filter), after 2 ms filter in which 2-ms bin was deleted in 8-ms interval (the interval corresponding to the frequency of DBS) and gap was merged, and after 2 s filter in which 2-s segments were selected and merged together in 5-s interval (the interval corresponding to 3-s on–2-s off stimulation cycles in DBS trials). Final length of three datasets after filter was identical at 60 s. A significant increase in burst rate appeared in the dataset underwent 2-ms filter in both STN and GP groups. Two-second filter, on the other hand, did not change the burst rate significantly in comparison with raw data ($^*P < 0.05$, $^{**}P < 0.01$, ANOVA test).

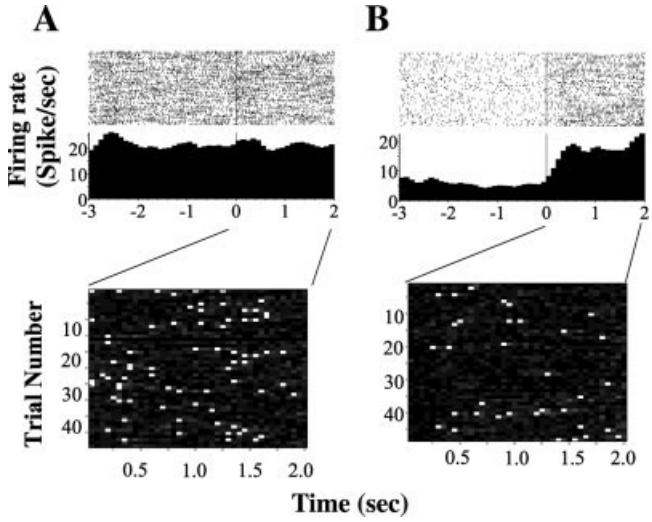

Fig. 8. Decreased burst firing during the 2-s stimulation-off period in the STN stimulation site. (**A**) Firing rate (top panel) and burst activity (bottom panel) in control condition without DBS. The plot was made using events created at 130/s (same as DBS frequency) as reference. Two-second segments were selected to calculate burst activity (marked by bright spots). (**B**) Neural activity and burst firing of the same neuron during behaviorally effective HFS. The firing rate was substantially reduced during 3-s stimulation-on period and returned to control level during 2-s stimulation-off period (top panel). The occurrence of burst spikes (bright spots) was reduced substantially during 2-s stimulation-off period (bottom panel) in comparison with that in control condition.

STN. Several clinical studies have indicated that unilateral DBS of the STN exerts bilateral beneficial effects on Parkinson's symptoms (Bastian et al., 2003; Chung et al., 2005; Germano et al., 2004; Linazasoro et al., 2003). A similar inhibitory effect found here in the contralateral STN may provide neural substrate for such bilateral beneficial effects.

Neural responses in the afferent (from the GP) and efferent (to the SNr) regions of the STN are of great significance, since such responses reflect direct impacts of DBS on the BG circuitry. We found a mixture of responses in both the GP (rodent equivalent of primate GPe) and the SNr during HFS of the STN; nearly equal number of neurons exhibited excitatory and inhibitory responses in these regions. It is well known that reciprocal projections exist between the GP and STN (Kita and Kitai, 1994; Sato et al., 2000). Thus, STN stimulation may induce both antidromic and orthodromic activation of GP cells. Short latency responses of ~1 ms (Kita and Kitai, 1991), suspected to occur in a subset of these neurons, would likely be obscured by stimulation artifact. The excitatory responses observed in the present study may be the result of longer latency antidromic responses or orthodromic activation of glutamatergic terminals of STN cells. The inhibitory responses in GP cells may be induced by the activation of inhibitory collaterals or by multiple synaptic actions via SNr or STR inputs (Chang et al., 1981; Wilson et al., 1982).

The SNr is a BG output nucleus that receives glutamatergic input from the STN and GABAergic input from the STR and GP. Contradictory results have been reported in regard to the effects of STN-DBS on this output nucleus: Inhibitory responses were found in these regions in anesthetized rats (Benazzouz et al., 1995, 2000), while increased GPi spike activity was observed in a study of awake, behaving primates with Parkinsonism (Hashimoto et al., 2003). Another primate study of GP HFS revealed either time-locked increases in firing rate or outright inhibition of the GP neurons (Bar-Gad et al., 2004). In the present study, we observed a mixture of SNr neuronal responses and a general, though not significant, increase in the mean firing rate. It should be noted that such responses, like those in the study by Hashimoto et al., were elicited by specific stimulation parameters that induced significant motor improvements without visible side effects.

The existence of both excitatory and inhibitory responses and increase in mean firing rate in SNr neurons does not fit well into any simple model of uniformed activation. Excitatory responses in the SNr may result from the HFS-induced activation of axons of STN neurons, even though HFS may simultaneously inhibit cell bodies (McIntyre and Grill, 1999). Inhibitory responses in the SNr could be attributed to the activation of inhibitory intranigral axon collaterals (Deniau et al., 1982; Mailly et al., 2003) and to the reduction of subthalamonigral glutamatergic inputs, depending on the distance between the fibers and the stimulation electrodes. In fact, Maurice et al. (2003) recently demonstrated in anesthetized rats that both excitatory and inhibitory responses were elicited in the SNr by STN HFS, and

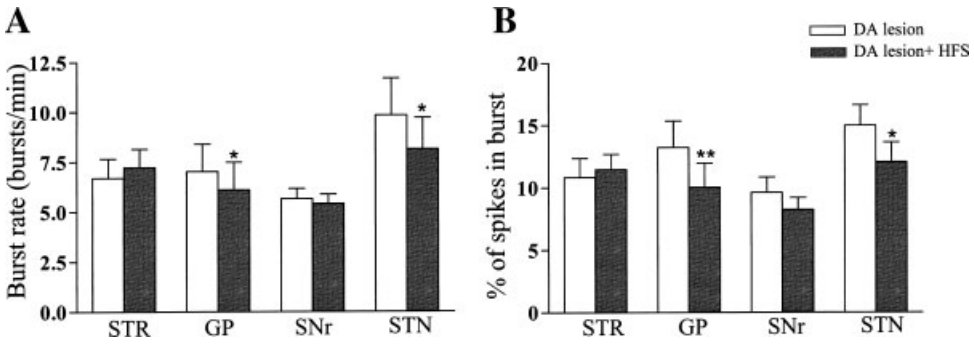

Fig. 9. Changes in burst firing in different regions of the BG during behaviorally effective DBS. Significant decreases in burst firing rate (**A**) and % of spikes in burst (**B**) were found in the ipsilateral GP and STN during 2-s stimulation-off periods of the HFS cycle.

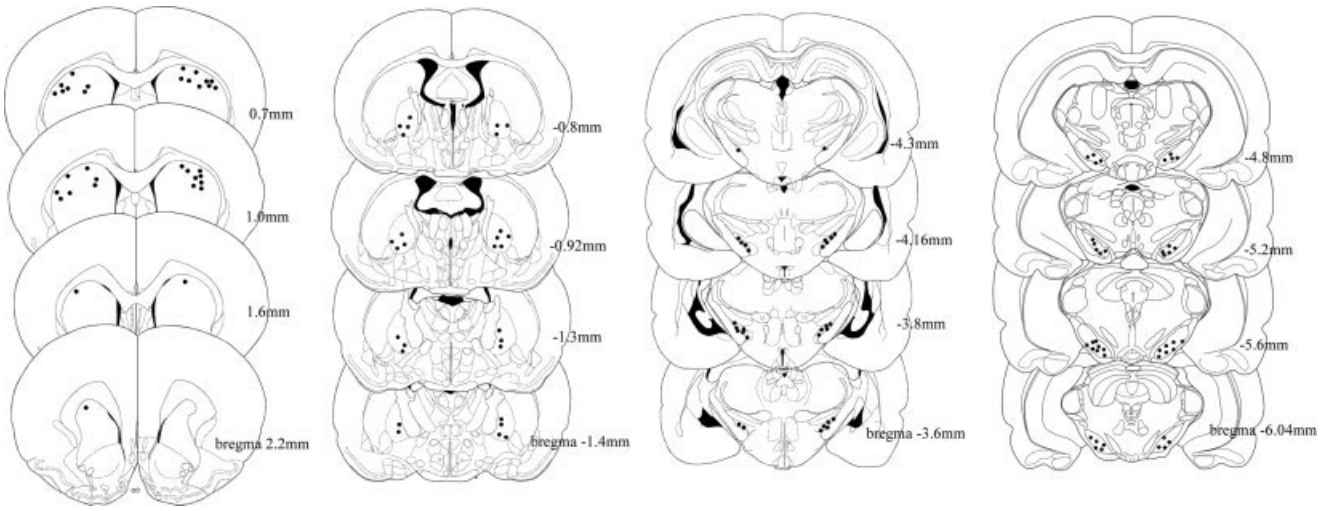

Fig. 10. Histological localization of recording sites in different BG regions. Results presented in this report came from these electrodes located correctly within corresponding structures.

that the direction of the response was dependent upon the stimulation intensity. That is, low intensity stimulation (<300 μA) induced inhibitory responses, while high intensity stimulation induced excitatory responses. We found both excitatory and inhibitory responses with behaviorally effective stimulation intensity that was less than 200 μA. Differences in animal models (e.g., anesthetized vs. awake) make it difficult to compare directly the stimulation parameters between these two studies. Nevertheless, the mixture of SNr neuronal responses found in our study suggests that DBS does not uniformly change discharge rates of BG output sites.

Neural responses in the STR, an input region of the BG circuit, can result from either direct stimulation of striatonigral fibers passing through the STN (Hammond et al., 1978) or the activation of corticostriatal pathway by the indirect action of cortical neurons. A moderate projection from the STN to the STR may also be responsible for orthodromic activation of STR cells (Kitai and Kita, 1987; Parent and Hazrati, 1995; Smith et al., 1990). Long latency responses, on the other hand, may result from feedback activity from downstream regions such as the GP, thalamus, and cortex, since all of these regions send projections to the STR (Castle et al., 2005; McFarland and Haber, 2000; Rudkin and Sadikot, 1999; Walker et al., 1989; Wright et al., 1999).

Changes in neural firing patterns are implicated in BG information processing, and alterations in burst firing patterns have been observed in the BG in primate PD models and in human with PD (Hurtado et al., 2005; Levy et al., 2000; Nini et al., 1995; Raz et al., 2000, 2001). In the present study, we examined changes in burst firing patterns within the BG during behaviorally effective HFS of the STN. Owing to the prevalent stimulation artifacts, analysis of burst firing during HFS is not feasible. However, we noted that the improved motor benefit lasted beyond the stimulation periods, and we thus analyzed data collected during the 2-s off interstimulation intervals of the HFS cycles. This approach allows us to detect burst patterns in the absence of stimulation artifacts during a time at which the behavioral effects of DBS are apparent. Obvious caveats need to be considered in that the analysis was not performed during DBS and important changes during the stimulation period could have been missed. Nevertheless, decreased burst firing was found in the GP and the STN, whereas no changes were

detected in the STR and SNr. Significant decreases in burst firing in the GP (where antidromic activation may occur) and in the STN (where the HFS was delivered) are to be expected. And this direct action may exert long-lasting effects that extend well into the 2-s stimulation-off period. Failure to detect changes in the SNr and STR, on the other hand, could be the result of short-lasting effects or indirect actions of STN-DBS. Thus, the negative results in the STR and SNr do not exclude the possibility that altered burst firing does occur during the HFS period.

In summary, the present study examined the neural responses in the major BG regions during behaviorally effective DBS of the STN in a rat model of PD. A simple model is that DBS inhibits neurons within the subthalamic stimulation site and reduces burst firing in the STN and GP. The effects of DBS on firing rate in other BG regions, however, are more complex. Effects appear to persist, as altered bursting in GP and STN, into the intervals between stimulation. These results suggest that the effect of DBS is likely to change firing patterns within the cortical BG system, besides inducing simple inhibition or excitation of the BG cells.

ACKNOWLEDGMENTS

We thank Ms. Hue-Ming Ding and Mr. Darrell Agee for technical assistance. This manuscript was revised by a professional scientific editor in association with Write Science Right.

REFERENCES

Albin RL, Young AB, Penney JB. 1989. The functional anatomy of basal ganglia disorders. Trends Neurosci 12:366–375.

Alexander GE, Crutcher MD, Delong MR. 1990. Basal ganglia-thalamocortical circuits: Parallel substrates for motor, oculomotor, "prefrontal" and "limbic" functions. Prog Brain Res 85:119–146.

Anderson ME, Postupna N, Ruffo M. 2003. Effects of high-frequency stimulation in the internal globus pallidus on the activity of thalamic neurons in the awake monkey. J Neurophysiol 89:1150–1160.

Ashkan K, Wallace B, Bell BA, Benabid AL. 2004. Deep brain stimulation of the subthalamic nucleus in Parkinson's disease 1993–2003: Where are we 10 years on? Br J Neurosurg 18:19–34.

Bar-Gad I, Elias S, Vaadia E, Bergman H. 2004. Complex locking rather than complete cessation of neuronal activity in the globus pallidus of a 1-methyl-4-phenyl-1,2,3,6-tetrahydropyridine-treated primate in response to pallidal microstimulation. J Neurosci 24: 7410–7419.

Bastian AJ, Kelly VE, Revilla FJ, Perlmutter JS, Mink JW. 2003. Different effects of unilateral versus bilateral subthalamic nucleus stimulation on walking and reaching in Parkinson's disease. Mov Disord 18:1000–1007.

Benabid AL, Benazzous A, Pollak P. 2002. Mechanisms of deep brain stimulation. Mov Disord 17 (Suppl. 3):S73–S74.

Benazzouz A, Piallat B, Pollak P, Benabid AL. 1995. Responses of substantia nigra pars reticulata and globus pallidus complex to high frequency stimulation of the subthalamic nucleus in rats: Electrophysiological data. Neurosci Lett 189:77–80.

Benazzouz A, Gao DM, Ni ZG, Piallat B, Bouali-Benazzouz R, Benabid AL. 2000. Effect of high-frequency stimulation of the subthalamic nucleus on the neuronal activities of the substantia nigra pars reticulata and ventrolateral nucleus of the thalamus in the rat. Neuroscience 99:289–295.

Beurrier C, Bioulac B, Audin J, Hammond C. 2001. High-frequency stimulation produces a transient blockade of voltage-gated currents in subthalamic neurons. J Neurophysiol 85:1351–1356.

Brown P. 2003. Oscillatory nature of human basal ganglia activity: Relationship to the pathophysiology of Parkinson's disease. Mov Disord 18:357–363.

Castle M, Aymerich MS, Sanchez-Escobar C, Gonzalo N, Obeso JA, Lanciego JL. 2005. Thalamic innervation of the direct and indirect basal ganglia pathways in the rat: Ipsi- and contralateral projections. J Comp Neurol 483:143–153.

Chang HT, Wilson CJ, Kitai ST. 1981. Single neostriatal efferent axons in the globus pallidus: A light and electron microscopic study. Science 213:915–918.

Chang JY, Shi LH, Luo F, Woodward DJ. 2003. High frequency stimulation of the subthalamic nucleus improves treadmill locomotion in unilateral 6-hydroxydopamine lesioned rats. Brain Res 983:174–184.

Chang JY, Shi LH, Luo F, Woodward DJ. 2006. Neural responses in multiple basal ganglia regions following unilateral dopamine depletion in spontaneous and treadmill locomotion tasks. Exp Brain Res (in press).

Chung SJ, Jeon SB, Im JH, Kim SR, Lee MC. 2005. Bilateral improvement after unilateral subthalamic nucleus stimulation in a patient with advanced Parkinson's disease. Mov Disord 20:S71–S72.

Cohen AH, Gans C. 1975. Muscle activity in rat locomotion: Movement analysis and electromyography of the flexors and extensors of the elbow. J Morphol 146:177–196.

DeLong MR. 1990. Primate models of movement disorders of basal ganglia origin. Trends Neurosci 13:281–285.

Deniau JM, Kitai ST, Donoghue JP, Grofova I. 1982. Neuronal interactions in the substantia nigra pars reticulata through axon collaterals of the projection neurons. An electrophysiological and morphological study. Exp Brain Res 47:105–113.

Do MTH, Bean BP. 2003. Subthreshold sodium currents and pacemaking of subthalamic neurons: Modulation by slow inactivation. Neuron 39:109–120.

Dostrovsky JO, Lozano AM. 2002. Mechanisms of deep brain stimulation. Mov Disord 17:S63–S68.

Dostrovsky JO, Hutchison WD, Lozano AM. 2002. The globus pallidus, deep brain stimulation, and Parkinson's disease. Neuroscientist 8:284–290.

Durif F, Lemaire JJ, Debilly B, Dordain G. 2002. Long-term follow-up of globus pallidus chronic stimulation in advanced Parkinson's disease. Mov Disord 17:803–807.

Filali M, Hutchison WD, Palter VN, Lozano AM, Dostrovsky JO. 2004. Stimulation-induced inhibition of neuronal firing in human subthalamic nucleus. Exp Brain Res 156:274–281.

Garcia L, Audin J, D'Alessandro G, Bioulac B, Hammond C. 2003. Dual effect of high-frequency stimulation on subthalamic neuron activity. J Neurosci 23:8743–8751.

Germano IM, Gracies JM, Weisz DJ, Tse W, Koller WC, Olanow CW. 2004. Unilateral stimulation of the subthalamic nucleus in Parkinson disease: A double-blind 12-month evaluation study. J Neurosurg 101:36–42.

Goldberg JA, Rokni U, Boraud T, Vaadia E, Bergman H. 2004. Spike synchronization in the cortex-basal ganglia networks of parkinsonian primates reflects global dynamics of the local field potentials. J Neurosci 24:6003–6010.

Hammond C, Deniau JM, Rizk A, Feger J. 1978. Electrophysiological demonstration of an excitatory subthalamonigral pathway in the rat. Brain Res 151:235–244.

Hashimoto T, Elder CM, Okun MS, Patrick SK, Vitek JL. 2003. Stimulation of the subthalamic nucleus changes the firing pattern of pallidal neurons. J Neurosci 23:1916–1923.

Hurtado JA, Rubchinsky LL, Sigvardt KA, Wheelock VL, Pappas CTE. 2005. Temporal evolution of oscillations and synchrony in GPi/muscle pairs in Parkinson's disease. J Neurophysiol 93:1569–1584.

Kita H, Kitai ST. 1991. Intracellular study of rat globus pallidus neurons: Membrane properties and responses to neostriatal, subthalamic and nigral stimulation. Brain Res 564:296–305.

Kita H, Kitai ST. 1994. The morphology of globus pallidus projection neurons in the rat: An intracellular staining study. Brain Res 636: 308–319.

Kitai ST, Kita H. 1987. Anatomy and physiology of the subthalamic nucleus: A driving force of the basal ganglia. In: Carpenter MB, Jayaraman A, editors. Basal Ganglia II, Vol. 32. New York: Plenum. p 357–373.

Lee KH, Roberts DW, Kim U. 2003. Effect of high-frequency stimulation of the subthalamic nucleus on subthalamic neurons: An intracellular study. Stereotact Funct Neurosurg 80:32–36.

Legendy CR, Salcman M. 1985. Burst and recurrences of burst in the spike trains of spontaneously active striate cortex neurons. J Neurophysiol 53:926–939.

Levy R, Hutchison WD, Lozano AM, Dostrovsky JO. 2000. High-frequency synchronization of neuronal activity in the subthalamic nucleus of parkinsonian patients with limb tremor. J Neurosci 20: 7766–7775.

Linazasoro G, Van BN, Lasa A. 2003. Unilateral subthalamic deep brain stimulation in advanced Parkinson's disease. Mov Disord 18: 713–716.

Lozano AM, Dostrovsky J, Chen R, Ashby P. 2002. Deep brain stimulation for Parkinson's disease: Disrupting the disruption. Lancet Neurol 1:225–231.

Magarinos-Ascone C, Pazo JH, Macadar O, Buno W. 2002. High-frequency stimulation of the subthalamic nucleus silences subthalamic neurons: A possible cellular mechanism in Parkinson's disease. Neuroscience 115:1109–1117.

Mailly P, Charpier S, Mentrey A, Deniau JM. 2003. Three-dimensional organization of the recurrent axon collateral network of the substantia nigra pars reticulata neurons in the rat. J Neurosci 23:5247–5257.

Maurice N, Thierry AM, Glowinski J, Deniau JM. 2003. Spontaneous and evoked activity of substantia nigra pars reticulata neurons during high-frequency stimulation of the subthalamic nucleus. J Neurosci 23:9929–9936.

McFarland NR, Haber SN. 2000. Convergent inputs from thalamic motor nuclei and frontal cortical areas to the dorsal striatum in the primate. J Neurosci 20:3798–3813.

McIntyre CC, Grill WM. 1999. Excitation of central nervous system neurons by nonuniform electric fields. Biophys J 76:878–888.

Meissner W, Leblois A, Hansel D, Bioulac B, Gross CE, Benazzouz A, Boraud T. 2005. Subthalamic high frequency stimulation resets subthalamic firing and reduces abnormal oscillations. Brain 128: 2372–2382.

Nini A, Feingold A, Slovin H, Bergman H. 1995. Neurons in the globus pallidus do not show correlated activity in the normal monkey, but phase-locked oscillations appear in the MPTP model of parkinsonism. J Neurophysiol 74:1800–1805.

Parent A, Hazrati L-N. 1995. Functional anatomy of the basal ganglia. I. The cortico-basal ganglia-thalamo-cortical loop. Brain Res Rev 20:91–127.

Paxinos G, Watson C. 1986. The Rat Brain in Stereotaxic Coordinates. San Diego: Academic Press.

Raz A, Vaadia E, Bergman H. 2000. Firing patterns and correlations of spontaneous discharge of pallidal neurons in the normal and the tremulous 1-methyl-4-phenyl-1,2,3,6-tetrahydropyridine vervet model of parkinsonism. J Neurosci 20:8559–8571.

Raz A, Frechter-Mazar V, Feingold A, Abeles M, Vaadia E, Bergman H. 2001. Activity of pallidal and striatal tonically active neurons is correlated in mptp-treated monkeys but not in normal monkeys. J Neurosci 21:RC128.

Rudkin TM, Sadikot AF. 1999. Thalamic input to parvalbumin-immunoreactive GABAergic interneurons: Organization in normal striatum and effect of neonatal decortication. Neuroscience 88: 1165–1175.

Sato F, Lavallee P, Levesque M, Parent A. 2000. Single-axon tracing study of neurons of the external segment of the globus pallidus in primate. J Comp Neurol 417:17–31.

Schultz W, Romo R. 1992. Role of primate basal ganglia and frontal cortex in the internal generation of movements. I. Preparatory activity in the anterior striatum. Exp Brain Res 91:363–384.

Shi LH, Woodward DJ, Luo F, Anstrom K, Schallert T, Chang JY. 2004. High-frequency stimulation of the subthalamic nucleus reverses limb-use asymmetry in rats with unilateral 6-hydroxydopamine lesions. Brain Res 1013:98–106.

Smith Y, Hazrati LN, Parent A. 1990. Efferent projections of the subthalamic nucleus in the squirrel monkey as studied by the PHA-L anterograde tracing method. J Comp Neurol 294:306–323.

Tai CH, Boraud T, Bezard E, Bioulac B, Gross C, Benazzouz A. 2003. Electrophysiological and metabolic evidence that high-frequency stimulation of the subthalamic nucleus bridles neuronal activity in the subthalamic nucleus and the substantia nigra reticulata. FASEB J 17:1820–1830.

Vitek JL. 2002a. Deep brain stimulation for Parkinson's disease—A critical re-evaluation of STN versus GPi DBS. Stereotact Funct Neurosurg 78:119–131.

Vitek JL. 2002b. Mechanisms of deep brain stimulation: Excitation or inhibition. Mov Disord 17:S69–S72.

Walker RH, Arbuthnott GW, Wright AK. 1989. Electrophysiological and anatomical observations concerning the pallidostriatal pathway in the rat. Exp Brain Res 74:303–310.

Welter ML, Houeto JL, Bonnet AM, Bejjani PB, Mesnage V, Dormont D, Navarro S, Cornu P, Agid Y, Pidoux B. 2004. Effects of high-frequency stimulation on subthalamic neuronal activity in parkinsonian patients. Arch Neurol 61:89–96.

West MO, Carelli RM, Pomerantz M, Cohen SM, Gardner JP, Chapin JK, Woodward DJ. 1990. A region in the dorsolateral striatum of the rat exhibiting single-unit correlations with specific locomotor limb movements. J Neurophysiol 64:1233–1246.

Wichmann T, DeLong MR. 1999. Oscillations in the basal ganglia. Nature 400:621–622.

Wilson CJ, Chang HT, Kitai ST. 1982. Origins of postsynaptic potentials evoked in identified rat neostriatal neurons by stimulation in substantia nigra. Exp Brain Res 45:157–167.

Wright AK, Norrie L, Ingham CA, Hutton EA, Arbuthnott GW. 1999. Double anterograde tracing of outputs from adjacent "barrel columns" of rat somatosensory cortex. Neostriatal projection patterns and terminal ultrastructure. Neuroscience 88:119–133.